AJNR

MR imaging of acute spinal cord injury: results of an experimental study in dogs.

E Schouman-Claeys, G Frija, C A Cuenod, D Begon, F Paraire and V Martin

MR Imaging of Acute Spinal Cord Injury: Results of an Experimental Study in Dogs

E. Schouman-Claeys[1]
G. Frija[1]
C. A. Cuenod[1]
D. Begon[2]
F. Paraire[3]
V. Martin[2]

A weight-drop model was used to induce 16 acute lesions of varying severity in the spinal cords of eight mongrel dogs. The subsequent 3- to 7-hr postinjury MR images (0.5 T) were assessed. T1-weighted images contributed little information. Injection of gadolinium tetra-azacyclododecane tetraacetic acid did not result in significant enhancement. T2-weighted sequences offered precise detection and delineation of the lesions, displaying fusiform hyperintense signal abnormalities that corresponded to both edema and hemorrhage. In low-impact injuries, abnormalities were small and centrally located, sparing the periphery of the spinal cord. In these cases hemorrhage was minimal and limited to the center of the lesion. In severe-impact injuries, MR showed widespread longitudinal extension with involvement of the periphery of the spinal cord. In the most severe injuries, a central heterogeneous signal component was frequently observed opposite the site of impact because of important hemorrhage within the cord. Overall, hyperintense areas correlated closely with lesion severity, as demonstrated by pathologic findings.

T2-weighted MR images obtained at 0.5 T were found to be reliable in the evaluation of acute spinal cord trauma.

The potential of MR imaging in the assessment of spinal cord injuries has been demonstrated, mainly at high field strengths in a few animal studies [1, 2] and in some clinical series [3–7]. Still needing clarification are the value of intermediate field strengths and variations in lesion patterns according to the severity of injury, this being clearly detailed in only one clinical study [7]. Our experimental in vivo study was carried out on 16 lesions in eight dogs. The main objective was to determine the value of 0.5-T MR in demonstrating acute spinal cord injury (3–7 hr after injury). Other objectives were (1) to compare MR findings with pathologic data; (2) to develop MR criteria to measure the severity of injury; (3) to evaluate the contribution of fast T2-weighted vs long TE/long TR spin-echo (SE) techniques; and (4) to assess the efficacy of IV injection of a paramagnetic contrast material, gadolinium tetra-azacyclododecane tetraacetic acid (Gd-DOTA), in cord injuries.

Materials and Methods

Experimental Model

Sixteen lesions were induced in eight adult mongrel dogs weighing 14.5–23 kg (mean, 17.7 kg); two concomitant lesions spaced two to three vertebrae apart were induced in each animal, with the craniad lesion located at the level of T12. The animals remained under general anesthesia throughout the experiment (intramuscular acepromazine, 0.2 mg/kg, followed by IV thiopental, 10 mg/kg initial dose with additional doses during the course of the procedure). The dogs were intubated but were able to breathe spontaneously.

An acceleration compression mechanism was adopted according to the weight-drop model introduced by Allen [8–10]. First, the dura mater was exposed by laminectomy; peeling off of

epidural fat and hemostasis were accomplished by electrocoagulation and bone wax. Next, a falling weight was directed through a cylinder at the posterior surface of the dura mater and removed immediately on impact. This model made it possible to induce lesions of varying severity. Four increasing degrees of trauma graded from I to IV were each induced four times (Table 1). Two different degrees of trauma were induced in each dog.

Imaging Procedure

Imaging was performed with a 0.5-T supraconducting unit (Magniscan CGR). Animals were placed in the supine position in a rectangular-shaped spine surface coil with a 320- by 180-mm field of view. Analysis involved a 4-mm-thick midline sagittal section with a 256-mm field of view (voxel size, 1.09 × 1.09 × 4 mm). As a result of our preliminary observations, we did not use ECG gating, which shows little benefit when subarachnoid spaces are as small as in our animals; nor did we image in the transverse plane, as interpretation of these images is difficult owing to the small diameter of the spinal cord.

Three different sequences were evaluated: T1-weighted SE 300/26/2 (TR/TE/excitations); T2-weighted long TR/long TE SE 1800/60, 120, 180, 240/2; and fast T2-weighted SE 600/60, 120, 180, 240/2 with a 45° angle. Data acquisition times were 2 min 57 sec, 15 min 29 sec, and 5 min 7 sec, respectively.

The format for imaging was as follows: (1) initial T1- and T2-weighted sequences, (2) two sequential T1-weighted sequences during at least a 30-min interval following IV injection of Gd-DOTA (0.1 mmol/kg) and separated from each other by mean intervals of 90 min, and (3) final T2-weighted sequences.

The mean interval between lesion formation and the imaging procedure was 2 hr 30 min for the initial T1-weighted sequence, 3 hr for the initial T2-weighted SE sequence, 3 hr 15 min for the initial fast T2-weighted sequence, 4 hr for the first sequence after injection of Gd-DOTA, 5 hr 45 min for the second injection, and then 6 hr 30 min and 7 hr for the SE and fast T2-weighted sequences, respectively (time data correspond to the end of sequence acquisitions).

Pathology

Immediately after completion of the imaging procedure, animals were given overdose anesthesia (pentobarbital, 4 g) and the spinal cord and dura matter were excised. This material was fixed in 10% formalin and then embedded in paraffin. Blocks were sectioned longitudinally in the midsagittal plane. The study consisted of gross anatomic examination of this sagittal section and then, after hematoxylin and eosin staining, histologic analysis of sagittal sections.

The intensities of the two lesion components (hemorrhage and edema) were evaluated on histologic preparations for both the center

and periphery of the lesion by using a rating scale of 0–4 (0 = normal, 4 = severe abnormality). Edema was identified by conventional histopathologic criteria: dissociation of normal structures by a substance containing varying amounts of polynuclear and lymphocytic cells and fibrin. With fixed material, we were able to appreciate an increase in spinal cord volume or quantify edema. With thin slices we could not appreciate neuronal tract section.

Imaging Analysis

A consensus was required from two observers unaware of pathologic findings. Abnormal spinal cord signals were evaluated relative to normal spinal cord located in areas distant to the lesions. For each lesion and for each of the sequences, signal intensity was graded on a 0–4 scale (0 = normal, 4 = marked hyperintensity). Grades 3 and 4 were necessary to offer precise and reliable lesion delineation. Any signal heterogeneity was noted.

Lesion Extension

Lesion extension, assessed by gross pathologic examination and grades 3 and 4 MR images, was determined on the basis of two criteria: longitudinal extension (the result of absolute measurements in millimeters) and anteroposterior extension (graded on a scale of A–C: A = confined to the center of the spinal cord, B = greater extension and at its maximum extent when extending to the spinal cord periphery, and C = extensive involvement of spinal cord periphery).

Results

Pathology

Each lesion was identified and readily delineated on gross examination as a brownish area. The only exception to this was the smallest lesion in the series, which was punctate and hardly identifiable. Anteroposterior extension was determined in all 16 lesions, but longitudinal extension was assessed only in 15 lesions because two extensive lesions appeared to be confluent. The relationship between anteroposterior and longitudinal extension and trauma intensity is shown in Table 2.

The greater the degree of trauma, the more widespread was the extension in the craniocaudal and anteroposterior axes. However, the model did not provide perfect reproducibility, as extension of lesions in the longitudinal and anteroposterior axes was not identical when similar degrees of trauma were induced (Table 2). Therefore, according to the

TABLE 1: Summary of Procedure and Materials Used to Induce Experimental Spinal Cord Trauma in Dogs

Trauma Intensity Grade	No. of Experiments	Compression Force (g cm)	Energy (J/cm^2)	Mass (g)	Drop Height (cm)	Surface Area (cm^2)
I	4	300	0.08	15	20	0.38
II	4	600	0.15	15	40	0.38
III	4	2400	0.25	40	60	0.94
IV	4	2400	0.62	40	60	0.38

Note.—Four increasing degrees of trauma graded I–IV were induced four times in eight different animals. In grades I, II, and IV trauma, the weight dropped struck the dura matter directly, while in grade III lesions a semicylindrical plastic impounder was interposed on the surface of the dura matter.

TABLE 2: MR and Pathologic Findings in Experimentally Induced Spinal Cord Lesions in Dogs

Pathologic Classification/ Lesion No.	Trauma Intensity Grade	Extent on MR/Pathology Length (mm)	AP	Edema Center	Periphery	Hemorrhage Center	Periphery	T2	T1 (Control)	T1 (Contrast)	Central Abnormality on MR T2	T1
Minimal												
1	I	4/1	B/A	1	0	1	0	3	1	2	–	–
2	I	5/2	B/A	2	1	1	0	3	0[a]	0[a]	–	–
3	I	8/2.5	B/A	3	2	1	0	3	0	2	–	–
Moderate												
4	I	9/8	C/B	3	2	2	0	3	0	0	–	–
5	II	12/12	C/B	3	3	4	2	3	0[a]	0[a]	–	–
6	II	14/9	C/B	2	2	3	1	3	1	2	–	–
7	II	17/7	C/B	4	2	2	1	3	0	1	–	–
8	III	9/11	C/B	2	2	3	1	3	1	1	–	–
Severe												
9	II	12/11	C/C	3	2	3	2	3	0	1	Strong linear hyperintensity	–
10	III	12/7	C/C	2	2	3	1	3	0[a]	1	–	–
11	III	18/13	C/C	3	2	3	1	3	1	2	Punctate hypointensity	–
12	IV	18/17	C/C	2	2	3	2	3	0[a]	1	Strong linear hyperintensity bordered by two hypointense lines	–
13	IV	26/42	C/C	1	3	4	3	3	1	1	Punctate hypointensity	Linear hypointensity
14	IV	27/23	C/C	3	2	4	2	3	1	2	Strong linear hyperintensity and punctate hypointensity	Punctate hypointensity
15	III	90/84	C/C	3	2	4	2	3	1	2	–	–
16	IV	–[b]	C/C	3	2	3	1	3	1	2	Linear hypointensity within hyperintense area	–

Note.—The craniocaudal (length) and anteroposterior (AP) extents of lesions were assessed on T2-weighted MR images. AP rating: A = small lesions confined to the actual center of the spinal cord; B = greater extension, at maximum when juxtaposed with spinal cord periphery; C = extensive involvement of cord periphery. Edema and hemorrhage were rated on a 0–4 scale, where 0 = normal and 4 = severe abnormality. MR patterns were assessed on T2-weighted images (T2) and T1-weighted images (T1), both without contrast (control) and after IV injection of 0.1 mmol/kg Gd-DOTA: 0 = normal; 4 = marked hyperintensity.

[a] Refers to a moderate heterogeneous signal.

[b] Lesions 15 and 16 appeared to be confluent so there was only one longitudinal measurement for the two lesions.

trauma evaluated on pathologic specimens, lesions were classified as minimal, moderate, or severe (Table 2). Minimal lesions had grade A anteroposterior extension and were roundish (n = 3) (Figs. 1A and 1B, bottom). Moderate lesions had grade B anteroposterior extension and were ovoid with limited longitudinal extension (n = 5) (Figs. 1A and 1B, top). Severe lesions had grade C anteroposterior extension and widespread longitudinal extension (n = 8) (Fig. 2). Further discussion in this article will refer to this pathologic classification and not to trauma intensity. Whereas grade IV trauma induced severe lesions in all cases, grades III and II trauma caused moderate or severe lesions and grade I trauma induced minimal or moderate lesions (Table 2).

Lesions exhibited two concomitant features: hemorrhage and edema (Figs. 1A–1C and 2D). Their distribution (Table 2) was grossly the same, except that edema often extended beyond the hemorrhagic area, and, in moderate and severe lesions, stretched somewhat further away than the lesion area demarcated on gross examination. The intensity of the hemorrhage was always more pronounced in the center of the lesion than in the periphery, whereas edema was usually more homogeneous. The extent of hemorrhage, and more

precisely its extension and severity in the periphery of the lesion, appeared closely related to the severity of the lesion. Therefore, in minimal lesions the edematous component dominated over the hemorrhagic component.

MR Imaging

Signal pattern.—All lesions displayed on T2-weighted images were areas of abnormally strong hyperintensity (grade 3), very well delineated, centered on the site of impact, and extended in both cranial and caudal directions (Figs. 1D, 1E, 2C, and 3). On T1-weighted images, abnormalities were inconsistent, appearing as signal heterogeneity (4/16) or discrete hyperintensity (8/16) (Fig. 2A) at a signal level too low (intensity = 1) to allow reliable lesion delineation.

Moreover, in six of eight severe lesions a central area of abnormal signal was depicted opposite the site of impact and extending anteroposteriorly. This appearance was displayed mainly on T2-weighted images as a punctate or linear hypointense area (5/6) and/or a particularly strong, usually linear hyperintense area (grade 4) (4/6) (Fig. 2C). In two cases this abnormality was also shown on T1-weighted images (Fig. 2A)
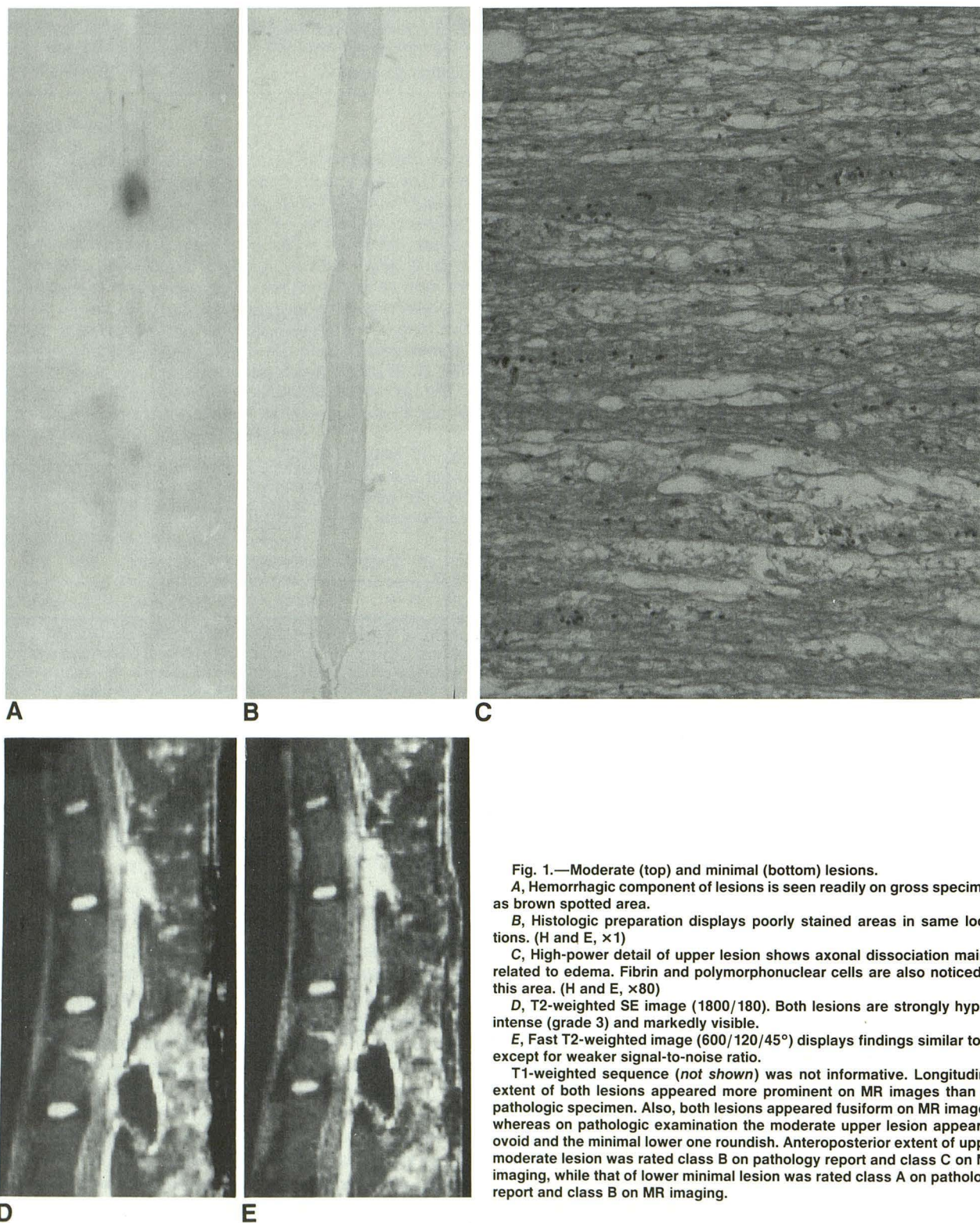
Fig. 1.—Moderate (top) and minimal (bottom) lesions.

A, Hemorrhagic component of lesions is seen readily on gross specimen as brown spotted area.

B, Histologic preparation displays poorly stained areas in same locations. (H and E, ×1)

C, High-power detail of upper lesion shows axonal dissociation mainly related to edema. Fibrin and polymorphonuclear cells are also noticed in this area. (H and E, ×80)

D, T2-weighted SE image (1800/180). Both lesions are strongly hyperintense (grade 3) and markedly visible.

E, Fast T2-weighted image (600/120/45°) displays findings similar to *D*, except for weaker signal-to-noise ratio.

T1-weighted sequence (*not shown*) was not informative. Longitudinal extent of both lesions appeared more prominent on MR images than on pathologic specimen. Also, both lesions appeared fusiform on MR images, whereas on pathologic examination the moderate upper lesion appeared ovoid and the minimal lower one roundish. Anteroposterior extent of upper moderate lesion was rated class B on pathology report and class C on MR imaging, while that of lower minimal lesion was rated class A on pathology report and class B on MR imaging.
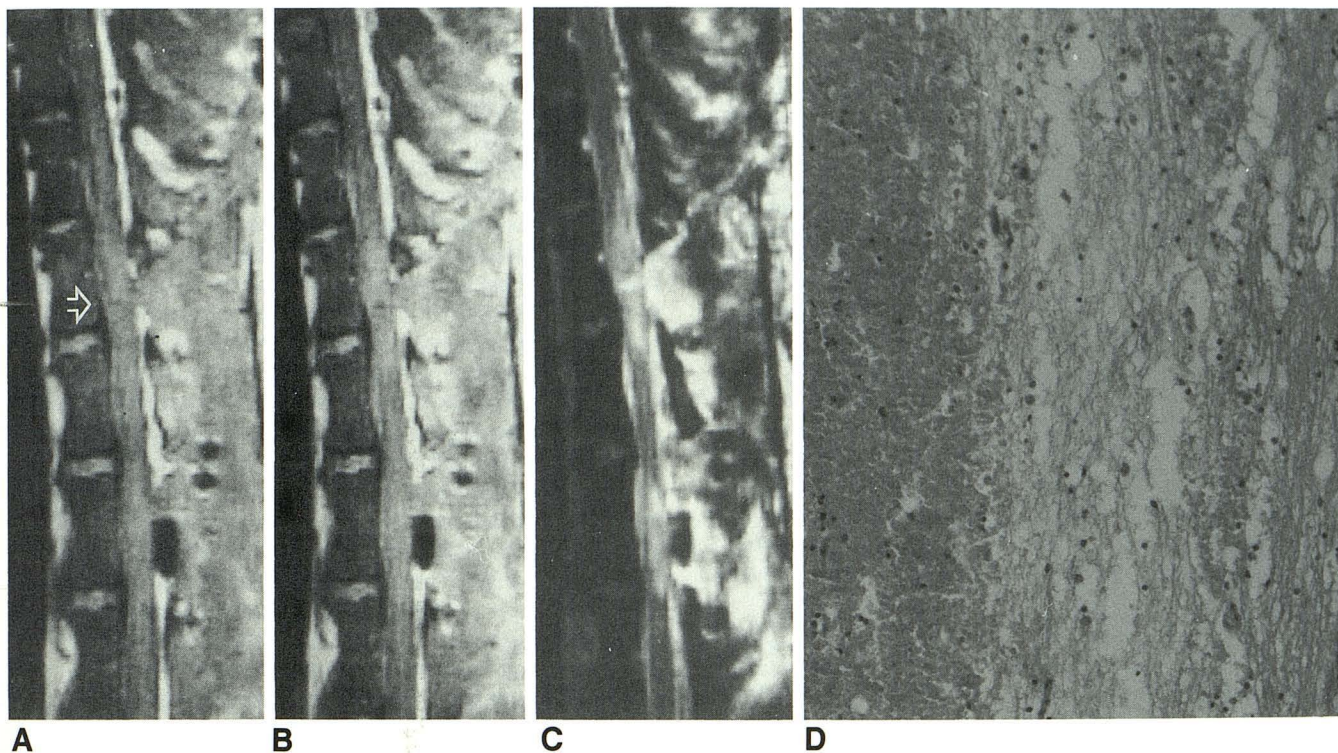
A   **B**   **C**   **D**

Fig. 2.—Severe lesions (top and bottom).

A, T1-weighted control image (300/26) shows fuzzy and poorly localized hyperintense areas (grade 1). Within center of upper lesion is punctate area of hypointensity (*arrow*). Both lesions contained hemorrhage, graded 4 in center and 2 in periphery of upper lesion, and 3 and 1, respectively, for lower lesion.

B, T1-weighted image after IV injection of Gd-DOTA. Both lesions were better evidenced (grade 2); nevertheless, enhancement was not sufficient to locate lesion precisely.

C, T2-weighted SE image (1800/180). Strong hyperintensity (grade 3) in both lesions provides precise demarcation of these fusiform lesions. Anteroposterior extent was graded C for both lesions on MR and pathologic specimen. Both lesions exhibited central abnormalities opposite area of impact: in upper lesion a particularly strong linear hyperintensity (grade 4) was associated with a punctate area of hypointensity; in lower lesion there was a punctate area of hypointensity.

D, High-power detail of upper lesion shows major axonal dissociation mainly related to extravasation of RBCs. Peripheral edema is seen also. (H and E, ×160)

as a small area of low signal. Results of individual studies are listed in Table 2.

Time course.—No signal abnormalities, as displayed on T2-weighted images, appeared to progress significantly during the course of the imaging procedure with respect to either morphology or intensity, except in one animal with two severe confluent lesions, a fact that was better seen at the end of the procedure. In that one case, delineation of the lesion was analyzed on the basis of the last T2-weighted SE sequence; others were analyzed on the T2-weighted scan with the highest signal.

Morphologic patterns.—Morphologic analysis was done on T2-weighted images. The three minimal lesions, and only these, were depicted on MR as limited fusiform hyperintense areas parallel to the axis of the spinal cord and localized in the center of the cord (lower lesions of Figs. 1D, 1E, and 3); their anteroposterior extension was limited (grade B). None of them displayed any localized abnormal component. Conversely, other lesions, both moderate or severe, had more widespread longitudinal extension (Table 2) and always involved the periphery of the spinal cord (grade C) (upper lesions on Figs. 1D, 1E, and 3 and both lesions of Fig. 2). Moreover,

most of the severe lesions, but only those, frequently had a central heterogeneous signal component opposite the site of impact.

Fast vs conventional T2-weighted SE sequences.—Fast T2-weighted sequences were evaluated in 10 lesions (four grade I trauma, four grade II trauma, one grade III trauma, and one grade IV trauma); although they generally exhibited lower signal compared with SE sequences, they exhibited findings similar to conventional SE sequences and were similarly graded (Figs. 1D and 1E).

Gd-DOTA injection.—Injection of Gd-DOTA did not contribute any useful information. In comparison with control T1-weighted images, enhancement after the first injection was observed in 11 of 16 cases, but the high signal was always lower than that obtained with T2-weighted sequences (Fig. 2B). Confidence in lesion delineation remained poor except in a single case following the second injection. This second injection improved lesion conspicuity in a total of three cases. Individual results are listed in Table 2.

Correlation between MR images and anatomy.—Overall, MR measurements were closely related to anatomic measurements (r = 0.94 for length data), though MR estimations
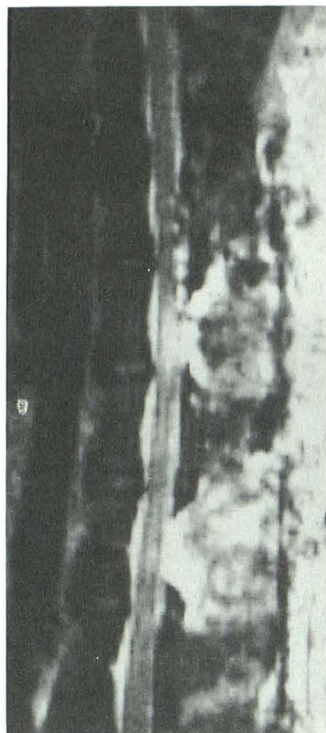
Fig. 3.—Moderate (top) and minimal (bottom) lesions. On T2-weighted SE image (1800/120), both lesions are clearly evidenced as a strong fusiform area of hyperintensity (grade 3). In upper lesion, extension to spinal cord periphery was considered to be more important on MR images (grade C) than on pathologic specimen (grade B). Similar findings were observed in lower lesion: On MR images the extent was graded B, whereas this lesion was barely depicted in pathologic and histologic examinations, evidenced as a central 1-mm lesion.

were usually superior to anatomic ones. Similar findings were noted along the anteroposterior axis: grade A extension on anatomic specimens was grade B on MR, grades B and C extension on anatomic specimens were grade C on MR. The findings that round minimal lesions on anatomic specimens appeared fusiform on MR images and that even the smallest lesion of the series was identified far more easily on MR than on both the gross and pathologic specimens corroborate these findings.

Discussion

Although the weight model that causes hemorrhagic necrotic spinal cord lesions is not a true replication of clinical spinal cord injury, it correlates best with the dynamics of human trauma. In accordance with data from the literature [11–16], lesions demonstrated a combination of hemorrhage and edema, the latter extending beyond the hemorrhage to varying degrees. Hemorrhage was more closely related to the severity of the lesion than edema was. Even limited lesions had a hemorrhagic component, whereas in clinical series they are often presumed to be only edematous [7]. Moreover, in contrast to one published experimental study [1], hemorrhage was not limited strictly to the center of the injury.

Within a relatively short time (3–7 hr) after injury, each lesion was seen as a very well-delineated homogeneous area of high signal on T2-weighted images. T1-weighted images displayed much less intense signal abnormalities and were thus much less informative. The hyperintensity on T2-weighted images is attributed to edema, which is known to

result in such MR abnormalities. The role of edema is also supported by the fact that the lesion extension was greater on T2-weighted images when compared with the anatomic specimens, while histopathologic techniques are relatively insensitive for demonstrating edema. However, hemorrhage, which was readily distinguishable on pathologic examination, might also be implicated, at least partly, for the high-signal abnormalities. Hemorrhage in the most acute phase (under 24 hr) has been reported, at 0.5 T [17] and 0.15 T [18], to induce a high signal, more pronounced on T2-weighted than on T1-weighted images. Thus, hemorrhage might also underlie the mild hyperintensity observed in half of the lesions on T1-weighted images, since a low signal would be expected for edema alone. The basis for the manifestations in hyperacute hemorrhage at 0.5 T is not well established. To explain the initially observed hyperintense signal on T2-weighted images, Zimmerman et al. [17] implicated the high water content of acute extravasated blood, and on T1-weighted images the high proton-density effects overwhelming the T1 prolongation effect. The difference between the results of our study and those of Gomori et al. [19] regarding the patterns of hemorrhage may be due to differences in field strength or to the fact that we studied more acute hemorrhage.

We also evaluated the relationship between the lesions actually induced and the forces of impact; however, the model we used was not perfectly reproducible. Differences in the force of experimental trauma or varying spinal cord resistances in different animals might be implicated. Nonreproducibility is reputed to be one of the major shortcomings of our experimental model [9, 10], although it is currently considered to be standard in spinal cord injury experiments. We suggest that this model should be used in comparative laboratory studies when quantifying lesion severity with MR.

Pathologic data supplemented the distinctive MR patterns of the various lesions and enabled us to establish criteria of severity: (1) substantial lesion extension along the longitudinal axis of the cord, (2) extensive involvement of the spinal cord periphery in the anteroposterior axis, and (3) central abnormal signal area opposite the impact. In contrast, less severe lesions were small, centrally located, and at most involved the spinal cord periphery only partially. The topography of the lesions was consistent with data from the literature [11–16], traumatic lesions being known to (1) involve primarily and more severely the central gray matter and (2) extend from that epicenter in both the transverse plane and longitudinal axis, depending on the increasing severity of the trauma and the interval following injury. Extension to the spinal cord periphery implies involvement of connecting pathways of white matter and a poor prognosis. MR evaluation of this type of peripheral extension would be most accurate in the axial plane. A central abnormal signal area was not seen consistently and was observed only in severe lesions. This was seen more frequently on T2- than on T1-weighted images, as a high- and/or low-signal area. It might reflect the large central hemorrhage that was noted on histologic preparations of these severe lesions. Deoxyhemoglobin within hypoxic but still intact RBCs may induce local magnetic field heterogeneity with subsequent T2 shortening [18]. Interestingly, the series

by Kulkarni et al. [7], reporting the poor prognostic value of central low-signal areas, corroborates our findings.

Although in our study MR appearance was related to lesion severity, no prognostic criteria were determined even though the lowest impact force (300 g cm) is known to result in reversible neurologic deficits in the same species [10, 11]. Correlations with subsequent damage, whether reversible or not, are only presumptive since we did not record spinal cord conduction and no follow-up data were available. Some reservations should be made before extrapolating these experimental results to human beings. Spinal cord trauma most commonly results from anterior compression lesions (bony fragments, disk, or epidural hematoma), which was not the case in our model. Regarding image definition, we may assume that we could obtain higher-quality images in human beings, whose spinal cord is significantly larger than the dog's. Finally, we should remember that even though the most important events following acute spinal cord injury occur within minutes to hours, pathologic changes progress in severity for as long as 1 week or more [12], and our study dealt only with initial damage.

The diagnostic contribution of fast T2-weighted images compared with conventional SE sequences was interesting. Despite its lower signal compared with long TR/long TE SE images, the low-angle SE sequence has the advantage of substantially reducing scanning time without perceptible loss of information. Indeed, the objection raised in the emergency clinical setting of long acquisition times with MR, therefore, becomes less of a problem. Gradient-echo techniques, which are more sensitive for visualization of blood, would presumably be useful in such an application; we did not use these sequences because of poor image quality compared with SE images.

IV injection of Gd-DOTA resulted in an inconsistent and modest enhancement that did not contribute to diagnosis. This minimal enhancement results from early local ischemia [11, 12, 15, 20, 21] caused by impairment of arterial and venous flow [21]. Such vascular disturbances have been detected within the first 5 min [15], persist for hours, and may prevent sufficient drug delivery.

In conclusion, this study demonstrated the contribution of 0.5-T MR in acute spinal cord trauma, providing direct visualization of spinal cord injury. Injury can be quantified by using criteria regarding lesion extension (in the spinal cord periphery and the craniocaudad direction) and imaging patterns such as a central heterogeneous signal component indicating more severe lesions. Such findings require T2-weighted images. We also found that fast T2-weighted sequences were as informative as long TE/long TR SE sequences.

REFERENCES

1. Hackney DB, Asato R, Joseph PM, et al. Hemorrhage and edema in acute spinal cord compression: demonstration by MR imaging. *Radiology* **1986**;161:387–390
2. Chakeres DW, Flickinger F, Bresnahan JC, et al. MR imaging of acute spinal cord trauma. *AJNR* **1987**;8:5–10
3. Kulkarni MV, McArdle CB, Kopanicky D, et al. Acute spinal cord injury: MR imaging at 1.5 T. *Radiology* **1987**;163:837–843
4. Mirvis SE, Geisler FH, Jelinek JJ, Joslyn JN, Gellad F. Acute cervical spine trauma: evaluation with 1.5-T MR imaging. *Radiology* **1988**;166:807–816
5. Tarr RW, Drolshagen LF, Kernier TC, Allen JH, Partain CL, James AE Jr. MR imaging of recent spinal trauma. *J Comput Assist Tomogr* **1987**;11(3):412–417
6. McArdle CB, Crofford MJ, Mirfakhraee M, Amparo EG, Calhoun JS. Surface coil MR of spinal trauma: preliminary experience. *AJNR* **1986**;7:885–893
7. Kulkarni MV, Bondurant FJ, Rose SL, Narayana PA. 1.5 Tesla magnetic resonance imaging of acute spinal trauma. *RadioGraphics* **1988**; 8:(6)1059–1082
8. Allen AR. Surgery of experimental lesion of spinal cord equivalent to crush injury of fracture dislocation of spinal column—a preliminary report. *JAMA* **1911**;57:878–880
9. Khan M, Griebel R. Acute spinal cord injury in the rat: comparison of three experimental techniques. *Can J Neurol Sci* **1983**;10(3):161–165
10. De La Torre JC. Spinal cord injury models. *Progr Neurobiol* **1984**; 22(4):289–344
11. De La Torre JC. Spinal cord injury. Review of basic and applied research. *Spine* **1981**;6(4):315–335
12. Ducker TB. Experimental injury of the spinal cord. In: Vinkun PJ, eds. *Handbook of clinical neurology*, vol. 25. *Injuries of the spine and spinal cord.* Amsterdam: North-Holland, **1976**:9–26
13. Ducker TB, Kindt GW, Kempe LC. Pathological findings in acute experimental spinal cord trauma. *J Neurosurg* **1971**;35:272–276
14. Nemecek S, Petr R, Suba P, Rozsival V, Melka O. Longitudinal extension of oedema in experimental spinal cord injury. Evidence for two types of post-traumatic oedema. *Acta Neurochir* (Wien) **1977**;37(7):7–15
15. Sasaki S. Vascular change in the spinal cord after impact injury in the rat. *Neurosurgery* **1982**;10:360–363
16. Yashon D, Bingham G, Faddoul EM, Hunt WE. Edema of the spinal cord following experimental impact trauma. *J Neurosurg* **1973**;38:693–697
17. Zimmerman RD, Heier LA, Snow RB, Liu DPC, Kelly AB, Deck MDF. Acute intracranial hemorrhage: intensity changes on sequential MR scans at 0.5 T. *AJNR* **1988**;9:47–57
18. Nose T, Enomoto T, Hyodo A, et al. Intracerebral hematoma developing during MR examination. *J Comput Assist Tomogr* **1987**;11:184–187
19. Gomori JM, Grossman RI, Goldberg HI, Zimmerman RA, Bilaniuk LT. Intracranial hematomas: imaging by high field MR. *Radiology* **1985**;157:87–89
20. Rivlin AS, Tator CH. Regional spinal cord blood flow in rats after severe cord trauma. *J Neurosurg* **1978**;49:844–853
21. Nelson E, Gertz D, Rennels ML, Ducker TB, Blaumanis OR. Spinal cord injury: the role of vascular damage in the pathogenesis of central hemorrhagic necrosis. *Arch Neurol* **1977**;34:332–333